

Reliability modeling and statistical inference of accelerated degradation data with memory effects and unit-to-unit variability

Shi-Shun Chen ^{a, b}, Xiao-Yang Li ^{a, b, *}, Wen-Rui Xie ^c

^a School of Reliability and Systems Engineering, Beihang University, Beijing 100191, China

^b Science and Technology on Reliability and Environmental Engineering Laboratory, Beijing 100191, China

^c School of Mathematics, Jilin University, Changchun 130012, China

Abstract

Accelerated degradation testing (ADT) is an effective way to evaluate the lifetime and reliability of highly reliable products. Markovian stochastic processes are usually applied to describe the degradation process. However, the degradation processes of some products are non-Markovian due to the interaction with environments. Besides, owing to the differences in materials and manufacturing processes, products from the same population exhibit diverse degradation paths. Motivated by this issue, an ADT model with memory effects and unit-to-unit variability (UtUV) is proposed in this article. The memory effect in the degradation process is captured by the fractional Brownian motion (FBM) and the UtUV is considered in the acceleration model. Then, the lifetime and reliability under the normal operating condition are presented. To give an accurate estimation of the memory effect, a statistical inference method is devised based on the expectation maximization (EM) algorithm. The effectiveness of the proposed method is verified by a simulation case and a microwave case. It is shown that the estimation of the memory effect obtained by the EM algorithm is much more accurate than the traditional method. Moreover, without considering UtUV in the ADT model, the estimation of the memory effect can be highly biased. The proposed ADT model is superior in both deterministic degradation trend predictions and degradation boundary quantification compared to existing models.

Keywords: Accelerated degradation testing; fractional Brownian motion; unit-to-unit variability; EM algorithm; memory effect; reliability estimation.

Highlights

- An ADT model with the memory effect and UtUV is developed.
- A statistical inference method is proposed based on the EM algorithm.
- Estimation of the memory effect can be highly biased for ADT models without UtUV.
- The proposed statistical method gives an accurate estimation of the memory effect.

1 Introduction

1.1 Motivation

With the continuous progress of design and manufacturing technology, modern products tend to have extremely high reliability and long lifetime. At this point, accelerated degradation testing (ADT) is always employed, in which degradation data are obtained under more severe stress conditions. By modeling ADT data, the lifetime and reliability of products under normal conditions can be extrapolated and the saving of cost and time can be achieved. In general, the commonly used degradation models for ADT modeling are stochastic process models [1]. For example, Charki et al. [2] carried out ADT on photovoltaic modules under three temperature and humidity levels and employed the Wiener process to inference its lifetime under normal conditions. Santini et al. [3] utilized the gamma process to characterize the threshold voltage degradation observed in a commercial SiC MOSFET at different temperature and gate voltage levels and assessed its reliability under normal conditions. Yan et al. [4] recorded the tensile force degradation of the flax fiber reinforced composite laminates under different temperature and humidity levels and evaluated its lifetime and reliability under normal conditions using the Tweedie exponential dispersion process. More related works on ADT modeling can be found in [5-7].

A reasonable description of the degradation process in ADT modeling is essential to ensure the credibility of the lifetime and reliability assessments. Most existing ADT models hold a general assumption that performance degradation is a memoryless Markovian process with independent increments. However, for real engineering products, such as batteries or blast furnace walls [8], degradation typically exhibits non-Markovian properties, i.e., the future degradation increment is influenced by the current or historical states. The origin of this phenomenon can be attributed to the interaction with environments [9]. Since traditional Markovian models are inherently memoryless, they fail to describe the degradation of such dynamic systems, leading to an imprecise lifetime and reliability assessments. Hence, building up an ADT model considering the non-Markovian degradation is essential for enabling more accurate extrapolation of lifetime and reliability.

1.2 Literature review

To describe the non-Markovian property of a degradation process, some research introduced a state-dependent function to quantify the influence of the current state on the degradation rate and established different transformed stochastic processes. For instance, Giorgio et al. [10] established the transformed gamma process and derived the conditional distribution of the first passage time. Following this, Giorgio and Pulcini [11] further proposed the transformed Wiener process to describe the non-Markovian degradation process with possibly negative increments. Also, the transformed inverse Gaussian process [12] and the transformed exponential dispersion process [13] were presented and the corresponding parameter estimation methods based on the Bayesian framework were developed. However, for the above transformed stochastic processes, selecting a sensible form for the state-dependent function is challenging in the absence of prior knowledge. Besides, they only focus on the influence of the current state on the future degradation increment, which may not be sufficient for describing the memory effects of the entire degradation path.

Different from the state-dependent function, fractional Brownian motion (FBM) serves as a proficient mathematical tool for modeling non-Markovian stochastic processes incorporating memory effects [14, 15]. In an FBM, the degree of memory effects can be simply quantified by the Hurst exponent. To this end, FBM has drawn much attention in degradation modeling for remaining useful life (RUL) prediction [16]. Xi et al. [17] first introduced the FBM to capture the memory effects in the degradation process and predicted the RUL of a turbofan engine. Afterward, Xi et al. [18] proposed an improved degradation model by considering both the memory effects and unit-to-unit variability (UtUV). Furthermore, Shao and Si [19] extended the degradation model based on the FBM by considering the measurement errors. Xi et al. [20] further developed a multivariate degradation model based on the FBM to describe multivariate stochastic degradation systems with memory effects. The above studies found that compared to the Wiener process-based degradation models, the FBM-based ones can help for obtaining more accurate RUL predictions when facing degradation with memory effects.

In terms of ADT modeling, Si et al [21] constructed an ADT model based on the FBM. Their results indicated that the FBM-based ADT model could give more credible reliability assessments than the Wiener process-based ones. However, the extrapolation accuracy of the ADT model depends not only on the precise description of the degradation process, but also on proper uncertainty quantification. In an ADT, we can observe that different items exhibit diverse degradation paths, denoted as UtUV. The author [22] and other scholars [23, 24] have shown that ignoring UtUV in ADT modeling results in unreliable reliability and lifetime assessments in practical applications. Unfortunately, the existing FBM-based ADT models ignore UtUV. Although Xi et al. [18] has proposed a FBM-based degradation model incorporating UtUV, their model failed to capture the effect of external stresses on degradation. Therefore, extrapolation of the product lifetime and reliability under other stress levels cannot be achieved.

Besides, for the ADT models with UtUV, it is always challenging to get a solution by direct constrained optimization of the overall likelihood function since the source of effect on degradation is diverse (e.g., external stresses, time and specific degradation rate). Therefore, if external stresses and UtUV are both considered in the FBM-based degradation model, the statistical inference method used in [18] and [21] is not applicable. In the literature, a two-step maximum likelihood estimation (MLE) method was generally used to estimate unknown parameters of the Wiener-process based ADT models with UtUV [25, 26]. However, the two-step MLE method maximizes two partial likelihood functions separately and fails to guarantee the maximization of the overall likelihood function. This exists a risk of deviating from the real law of actual degradation data when dealing with ADT models with UtUV, especially when the memory effect is incorporated. As demonstrated in the following Section 4.3.1, the estimation of the memory effect obtained by the two-step MLE is highly biased leading to misjudgment of the degradation law, which results in significant deviations in reliability evaluation results.

1.3 Work and contribution

Motivated by the above limitations, a comprehensive degradation model considering memory effects, UtUV and external stresses simultaneously is presented. Besides, a statistical inference method is proposed based on the expectation maximization (EM) algorithm [27], where the maximization of the overall likelihood function can be implemented.

The main contributions of this paper are summarized as follows:

- 1) An improved FBM-based degradation model is proposed for reliability estimation of ADT data with memory effects, in which the influence of external stresses are incorporated and the UtUV is quantified.
- 2) A statistical inference method is presented based on the EM algorithm, in which the accurate estimation of the memory effect is achieved by maximizing the overall likelihood function rather than maximizing two partial likelihood functions separately.

1.4 Overview

The organization of the paper is as follows. Firstly, Section 2 gives the preliminary about the FBM. Then, in Section 3, an ADT model with memory effects and UtUV is proposed, and a statistical inference method based on the EM algorithm is presented. After that, in Section 4 and Section 5, the practicability and the superiority of the proposed methodology are verified by a simulation case and an engineering case, respectively. Finally, we conclude our work in Section 6.

2 Preliminary to fractional Brownian motion

Let a standard FBM denoted by $B_H(t)$, for a given time $t \geq 0$, $B_H(t)$ can be defined as [28]:

$$B_H(t) = \frac{1}{\Gamma\left(H + \frac{1}{2}\right)} \int_{-\infty}^t W_H(t-r) dB(r), \quad (1)$$

where

$$W_H(t-r) = \begin{cases} (t-r)^{H-1/2}, & 0 \leq r \leq t \\ (t-r)^{H-1/2} - (-r)^{H-1/2}, & r < 0; \end{cases} \quad (2)$$

$\Gamma(\cdot)$ is a gamma function formulated by

$$\Gamma(x) = \int_0^{\infty} t^{x-1} e^{-t} dt; \quad (3)$$

$B(\cdot)$ represents the standard Brownian motion; and H is the Hurst exponent with the range of $(0, 1)$. For the standard FBM shown in (1), the autocorrelation function can be expressed by

$$E[B_H(t)B_H(r)] = \frac{1}{2} \left(t^{2H} + r^{2H} - |t-r|^{2H} \right). \quad (4)$$

It can be seen from equation (4) that the memory effect is determined by H . Depending on the value of H , there are three different cases [18]:

- 1) When $0 < H < 0.5$, the increments of FBM are negatively correlated, which implies that future increments tend to an opposite tendency of the previous direction and the increment process has short-term memory.
- 2) When $H = 0.5$, the FBM degenerates into the BM, and there is no memory effect in the increment process.
- 3) When $0.5 < H < 1$, the increments of FBM are positively correlated, which implies that future increments tend to follow the previous direction and the increment process has long-term memory.

We can see that the standard BM is a special case of the standard FBM. In addition, for $t \geq 0$, the standard FBM exhibits the following properties:

- 1) $B_H(0) = 0$;
- 2) $E[B_H(t)] = 0$ and $E[B_H^2(t)] = t^{2H}$;
- 3) $B_H(t) - B_H(r) \sim B_H(t-r)$ for any $r < t$;
- 4) $B_H(at) \sim a^H B_H(t)$ for $a > 0$.

3 Methodology

3.1 Model construction

In order to describe the non-Markovian degradation process with memory effects, a standard FBM shown in (1) is introduced to construct the ADT model as follows:

$$X(s, t) = f(s, t) + \sigma B_H(t), \quad (5)$$

where $X(\cdot)$ denotes the performance degradation amount; $f(\cdot)$ is a function of stress s and time t , which depicts the deterministic performance degradation trend; σ represents the diffusion coefficient.

Generally speaking, $f(\cdot)$ in (5) can be decoupled as a performance degradation rate function $e(s)$ (also known as the acceleration model) multiplied by a time scale function $\tau(t)$ [22], i.e.:

$$X(s, t) = e(s) \cdot \tau(t) + \sigma B_H(t), \quad (6)$$

where $\tau(t) = t^\beta$, $\beta > 0$ is a common assumption for the time-scale transformation function [26]. If $\beta = 1$, then it represents a linear degradation process, otherwise a nonlinear degradation process; $e(s)$ indicates the relationship between degradation rate and stress (also known as the acceleration model) [29].

In general, $e(s)$ is usually assumed as a log-linear function as follows [22]:

$$e(s) = \exp(\alpha_0 + \alpha_1 s^*), \quad (7)$$

where α_0 and α_1 are constant unknown parameters; s^* is the standardized stress. For different type of acceleration models, s^* can be calculated as [30]:

$$s^* = \begin{cases} \frac{1/s_0 - 1/s}{1/s_0 - 1/s_H}, & \text{Arrhenius model,} \\ \frac{\ln s - \ln s_0}{\ln s_H - \ln s_0}, & \text{Power law model,} \\ \frac{s - s_0}{s_H - s_0}, & \text{Exponential model,} \end{cases} \quad (8)$$

where s_0 denotes the normal stress level; s_H denotes the highest stress levels. The choice of acceleration models mainly depends on the type of accelerated stress. For instance, the Arrhenius model is adopted if the accelerated stress is temperature; if the accelerated stress is humidity, the Power law model is employed [31].

As aforementioned, the UtUV plays a significant role in ADT modeling. To be specific, for items under the same operating conditions, each item may have its own performance degradation rate due to manufacturing imperfections [22]. As a result, it is reasonable to deduce that each item has unique $e(s)$. Without loss of generality, we make the assumption that the degradation rates of various items adhere to

a normal probability distribution. Thus, (6) can be transformed as:

$$X(s, t) = e(s) \cdot \tau(t) + \sigma B_H(t), e(s) \sim N(\mu_e(s), \sigma_e^2(s)). \quad (9)$$

Given that $e(s)$ is a random variable, the degradation rate function in (7) can be reformulated, as indicated by [22]

$$e(s) = \exp(\alpha_0 + \alpha_1 s^*) = a \exp(\alpha_1 s^*), a \sim N(\mu_a, \sigma_a^2), \quad (10)$$

where $a = \exp(\alpha_0)$ is a random variable with a normal probability distribution, $\mu_a > 0$, $\sigma_a > 0$. Then, the distribution parameter $\mu_e(s)$ and $\sigma_e(s)$ can be expressed as:

$$\mu_e(s) = \mu_a \exp(\alpha_1 s^*), \sigma_e(s) = \sigma_a \exp(\alpha_1 s^*). \quad (11)$$

3.2 Lifetime distribution and reliability analysis

The main purpose of ADT is to extrapolate the lifetime and reliability of the product at normal stress s_0 by using the degradation data subjected to high stress levels. In accordance with the definition of reliability within belief reliability theory [32], a product is considered to fail when its performance margin less than 0. Since X denotes the performance degradation amount, the performance margin M can be defined as:

$$M(s, t) = X_{th} - X(s, t), \quad (12)$$

where X_{th} denotes the critical threshold of the degradation process. Then, the failure time T of a product can be expressed as:

$$T(s) = \inf \{t | M(s, t) < 0\}, \quad (13)$$

and the reliability of a product R can be expressed as:

$$R(s, t) = \Pr \{T(s) \geq t\}, \quad (14)$$

where $\Pr\{\cdot\}$ denotes the probability measure.

Due to the complexity of the model, it is difficult to derive an explicit expression for (13) and (14). To solve this problem, we employ the Monte Carlo (MC) method to calculate the lifetime distribution and reliability of a product under specified operating conditions. Algorithm 1 gives the detailed procedures of the MC method.

Algorithm 1: The MC method to calculate the product lifetime distribution and reliability under specified operating conditions

Step 1. Determine the model parameters $\hat{\theta} = [\hat{\mu}_a, \hat{\sigma}_a^2, \hat{\alpha}_1, \hat{\beta}, \hat{\sigma}^2, \hat{H}]^T$ based on the EM algorithm in the subsequent Section C;

Step 2. According to $\hat{\theta}$, simulate N degradation trajectories under specified stress s . The q -th degradation trajectory can be obtained as:

2.1 Simulate the q^{th} standard FBM $B_{H=\hat{H}}^q(t)$ using the FFT algorithm [33] (Detailed steps of the FFT algorithm can be found in [21]);

2.2 Generate a unit-specific a^q according to its distribution $N(\widehat{\mu}_a, \widehat{\sigma}_a^2)$;

2.3 Acquire the degradation trajectory as $X_q(s, t) = a^q \exp(\widehat{\alpha}_1 s^*) \cdot t^{\widehat{\beta}} + \widehat{\sigma} B_{H=\widehat{H}}^q(t)$.

Step 3. Calculate the product lifetime distribution and reliability under specified stress s :

3.1 Calculate the failure time of the N simulated degradation trajectories by applying (13), denoted as $T_q (1 \leq q \leq N)$;

3.2 Derive the empirical lifetime distribution of the product under stress s as

$$F(t | \widehat{\theta}, s) = \frac{1}{N} \sum_{q=1}^N 1_t(T_q); 1_t(T_q) = \begin{cases} 1, & \text{if } T_q \leq t \\ 0, & \text{otherwise} \end{cases};$$

3.3 Calculate the product reliability at the specific time t using (14).

3.3 Statistical inference

In this paper, we consider a constant stress ADT, which is generally used in practice. The observed ADT data x_{lij} is denoted as the j^{th} degradation value of unit i subjected to the l^{th} stress level, $l = 1, 2, \dots, k$, $i = 1, 2, \dots, n_l$, $j = 1, 2, \dots, m_{li}$, where k is the number of stress levels, n_l is the number of test items under the l^{th} stress level, and m_{li} denotes the number of measurements for unit i subjected to the l^{th} stress level. The corresponding measurement time is represented by t_{lij} . Hereby, the degradation observations

of the i^{th} item tested at l^{th} stress level can be denoted as $\mathbf{x}_{li} = [x_{li1}, x_{li2}, \dots, x_{lim_i}]^T$. Furthermore, we

define $\boldsymbol{\tau}_{li} = [\tau(t_{li1}), \tau(t_{li2}), \dots, \tau(t_{lim_i})]^T$ and $\mathbf{B}_H^{li} = [B_H(t_{li1}), B_H(t_{li2}), \dots, B_H(t_{lim_i})]^T$.

According to (9) and (10), the unknown parameters $\boldsymbol{\theta} = [\mu_a, \sigma_a^2, \alpha_1, \beta, \sigma^2, H]^T$ need to be determined. In this section, a statistical inference approach employing the EM algorithm is presented.

Since each product has a unique degradation rate, for the i^{th} item tested at l^{th} stress level, we have

$$\mathbf{x}_{li} = a_{li} \boldsymbol{\psi}_{li} + \sigma \mathbf{B}_H^{li}, \quad (15)$$

where

$$\boldsymbol{\psi}_{li} = \exp(\alpha_1 s_l^*) \boldsymbol{\tau}_{li}. \quad (16)$$

The basic idea of the EM algorithm involves replacing unobservable variables with their conditional expectations, where parameter updates at each step can be derived in a closed or simple form [34]. The EM algorithm mainly comprises two steps. Firstly, the expectation of the log-likelihood is calculated with respect to the latent variables, which is called the expectation-step (E-step). Then, the maximizer of this expected likelihood is identified, which is called the maximization step (M-step). These two steps are iteratively repeated until reaching a satisfactory level of convergence.

In (15), a_{li} is unobservable and need to be replaced. We denote $\boldsymbol{\Omega} = \{a_{11}, \dots, a_{1n_1}, a_{21}, \dots, a_{ln_l}\}$. Subsequently, when provided with the complete data including \mathbf{x} and $\boldsymbol{\Omega}$, we can formulate the complete log-likelihood function as:

$$\ln L(\boldsymbol{\theta}|\mathbf{x}, \boldsymbol{\Omega}) = \sum_{l=1}^k \sum_{i=1}^{n_l} \left[\ln p(\mathbf{x}_{li} | a_{li}, \boldsymbol{\theta}) + \ln p(a_{li} | \boldsymbol{\theta}) \right], \quad (17)$$

where $p(\mathbf{x}_{li} | a_{li}, \boldsymbol{\theta})$ denotes the probability density function (PDF) of x_{li} given a_{li} and $\boldsymbol{\theta}$; and $p(a_{li} | \boldsymbol{\theta})$ denotes the PDF of a_{li} given $\boldsymbol{\theta}$. According to the ADT models (9) and (11), (17) can be extended as:

$$\begin{aligned} \ln L(\boldsymbol{\theta}|\mathbf{x}, \boldsymbol{\Omega}) = & -\frac{1}{2} \sum_{l=1}^k \sum_{i=1}^{n_l} \left\{ m_{li} \ln(2\pi) + \ln |\boldsymbol{Q}_{li}| + (\mathbf{x}_{li} - a_{li} \boldsymbol{\psi}_{li})^T \boldsymbol{Q}_{li}^{-1} (\mathbf{x}_{li} - a_{li} \boldsymbol{\psi}_{li}) \right\} \\ & -\frac{1}{2} \sum_{l=1}^k \sum_{i=1}^{n_l} \left\{ \ln(2\pi) + \ln \sigma_a^2 + \frac{(a_{li} - \mu_a)^2}{\sigma_a^2} \right\}, \end{aligned} \quad (18)$$

where \boldsymbol{Q}_{li} is a $K_{li} \times K_{li}$ dimensional covariance matrix and its $(u, v)^{\text{th}}$ entry can be calculated by

$$(\boldsymbol{Q}_{li})_{uv} = \frac{\sigma^2}{2} \left(t_{liu}^{2H} + t_{liv}^{2H} - |t_{liu} - t_{liv}|^{2H} \right). \quad (19)$$

To facilitate the following statistical inference, a re-parameterization of the unknown parameters is performed by $\boldsymbol{\Sigma}_{li} = \frac{\boldsymbol{Q}_{li}}{\sigma^2}$. Then, (18) can be rewritten as:

$$\begin{aligned} \ln L(\boldsymbol{\theta}|\mathbf{x}, \boldsymbol{\Omega}) = & -\frac{1}{2} \sum_{l=1}^k \sum_{i=1}^{n_l} (m_{li} + 1) \ln(2\pi) - \frac{1}{2} \sum_{l=1}^k \frac{n_l}{2} \ln \sigma_a^2 - \frac{1}{2} \sum_{l=1}^k \sum_{i=1}^{n_l} \frac{m_{li} n_l}{2} \ln \sigma^2 \\ & -\frac{1}{2} \sum_{l=1}^k \sum_{i=1}^{n_l} \ln |\boldsymbol{\Sigma}_{ij}| - \frac{1}{2} \sum_{l=1}^k \sum_{i=1}^{n_l} \left[\frac{(\mathbf{x}_{li} - a_{li} \boldsymbol{\psi}_{li})^T \boldsymbol{\Sigma}_{li}^{-1} (\mathbf{x}_{li} - a_{li} \boldsymbol{\psi}_{li})}{\sigma^2} + \frac{(a_{li} - \mu_a)^2}{\sigma_a^2} \right]. \end{aligned} \quad (20)$$

Considering the update of $\boldsymbol{\theta}$ during the iterations in the EM algorithm, let $\boldsymbol{\theta}^{(p)} = \left[\mu_a^{(p)}, \sigma_a^{2(p)}, \alpha_1^{(p)}, \beta^{(p)}, \sigma^{2(p)}, H^{(p)} \right]^T$ represent the estimations in the p^{th} step. To calculate the expectation of the log-likelihood function (20), it is necessary to derive the first and second moments of a_{li} conditional on \mathbf{x}_{li} and $\boldsymbol{\theta}^{(p)}$. Notably, it is evident that the distribution of a_{li} conditional on \mathbf{x}_{li} and $\boldsymbol{\theta}^{(p)}$ maintains a normal distribution [35]. Within the Bayesian framework, the posterior distribution of a_{li} can be acquired as:

$$\begin{aligned}
& p(a_{li} | \mathbf{x}_{li}, \boldsymbol{\theta}^{(p)}) \propto p(\mathbf{x}_{li} | a_{li}, \boldsymbol{\theta}^{(p)}) p(a_{li} | \boldsymbol{\theta}^{(p)}) \\
& \propto \exp \left[-\frac{1}{2} \frac{(\mathbf{x}_{li} - a_{li} \boldsymbol{\psi}_{li}^{(p)})^T [\boldsymbol{\Sigma}_{li}^{(p)}]^{-1} (\mathbf{x}_{li} - a_{li} \boldsymbol{\psi}_{li}^{(p)})}{\sigma^{2(p)}} \right] \exp \left[-\frac{(a_{li} - \mu_a^{(p)})^2}{2\sigma_a^{2(p)}} \right] \\
& \propto \exp \left\{ -\frac{1}{2} \left[\left(\frac{[\boldsymbol{\psi}_{li}^{(p)}]^T [\boldsymbol{\Sigma}_{li}^{(p)}]^{-1} \boldsymbol{\psi}_{li}^{(p)}}{\sigma^{2(p)}} + \frac{1}{\sigma_a^{2(p)}} \right) a_{li}^2 - 2 \left(\frac{\mathbf{x}_{li}^T [\boldsymbol{\Sigma}_{li}^{(p)}]^{-1} \boldsymbol{\psi}_{li}^{(p)}}{\sigma^{2(p)}} + \frac{\mu_a^{(p)}}{\sigma_a^{2(p)}} \right) a_{li} \right] \right\} \\
& \propto \exp \left[-\frac{\left[a_{li} - \left(\mathbf{x}_{li}^T [\boldsymbol{\Sigma}_{li}^{(p)}]^{-1} \boldsymbol{\psi}_{li}^{(p)} \sigma_a^{2(p)} + \mu_a^{(p)} \sigma^{2(p)} \right) / \left([\boldsymbol{\psi}_{li}^{(p)}]^T [\boldsymbol{\Sigma}_{li}^{(p)}]^{-1} \boldsymbol{\psi}_{li}^{(p)} \sigma_a^{2(p)} + \sigma^{2(p)} \right) \right]^2}{2\sigma^{2(p)} \sigma_a^{2(p)} / \left([\boldsymbol{\psi}_{li}^{(p)}]^T [\boldsymbol{\Sigma}_{li}^{(p)}]^{-1} \boldsymbol{\psi}_{li}^{(p)} \sigma_a^{2(p)} + \sigma^{2(p)} \right)} \right] \\
& \sim N\left(\mu_{li}^{(p)}, \sigma_{li}^{2(p)}\right)
\end{aligned} \tag{21}$$

with

$$\mu_{li}^{(p)} = \frac{\mathbf{x}_{li}^T [\boldsymbol{\Sigma}_{li}^{(p)}]^{-1} \boldsymbol{\psi}_{li}^{(p)} \sigma_a^{2(p)} + \mu_a^{(p)} \sigma^{2(p)}}{[\boldsymbol{\psi}_{li}^{(p)}]^T [\boldsymbol{\Sigma}_{li}^{(p)}]^{-1} \boldsymbol{\psi}_{li}^{(p)} \sigma_a^{2(p)} + \sigma^{2(p)}}, \tag{22}$$

$$\sigma_{li}^{2(p)} = \frac{\sigma^{2(p)} \sigma_a^{2(p)}}{[\boldsymbol{\psi}_{li}^{(p)}]^T [\boldsymbol{\Sigma}_{li}^{(p)}]^{-1} \boldsymbol{\psi}_{li}^{(p)} \sigma_a^{2(p)} + \sigma^{2(p)}}. \tag{23}$$

Subsequently, we employ the EM algorithm to estimate $\boldsymbol{\theta}$ iteratively. Firstly, the expectation $Q(\boldsymbol{\theta} | \mathbf{x}, \boldsymbol{\theta}^{(p)})$ of $\ln L(\boldsymbol{\theta} | \mathbf{x}, \boldsymbol{\Omega})$ with regard to $\boldsymbol{\Omega}$ is computed in the E-step. According to (20), (22) and (23), we can get

$$\begin{aligned}
Q(\boldsymbol{\theta} | \mathbf{x}, \boldsymbol{\theta}^{(p)}) &= E_{\boldsymbol{\Omega} | \boldsymbol{\theta}^{(p)}}[\ln L(\boldsymbol{\theta} | \mathbf{x}, \boldsymbol{\Omega})] \\
&= -\frac{1}{2} \sum_{l=1}^k \sum_{i=1}^{n_l} (m_{li} + 1) \ln(2\pi) - \frac{1}{2} \sum_{l=1}^k \frac{n_l}{2} \ln \sigma_a^2 - \frac{1}{2} \sum_{l=1}^k \sum_{i=1}^{n_l} \frac{m_{li} n_l}{2} \ln \sigma^2 \\
&\quad - \frac{1}{2} \sum_{l=1}^k \sum_{i=1}^{n_l} \ln |\boldsymbol{\Sigma}_{li}| - \frac{1}{2} \sum_{l=1}^k \sum_{i=1}^{n_l} \frac{\left[\mu_{li}^{(p)} \right]^2 + \sigma_{li}^{2(p)} - 2\mu_{li}^{(p)} \mu_a + \mu_a^2}{\sigma_a^2} \\
&\quad - \frac{1}{2} \sum_{l=1}^k \sum_{i=1}^{n_l} \frac{\mathbf{x}_{li}^T \boldsymbol{\Sigma}_{li}^{-1} \mathbf{x}_{li} - 2\mu_{li}^{(p)} \mathbf{x}_{li}^T \boldsymbol{\Sigma}_{li}^{-1} \boldsymbol{\psi}_{li} + \left(\left[\mu_{li}^{(p)} \right]^2 + \sigma_{li}^{2(p)} \right) \boldsymbol{\psi}_{li}^T \boldsymbol{\Sigma}_{li}^{-1} \boldsymbol{\psi}_{li}}{\sigma^2}.
\end{aligned} \tag{24}$$

In the M-step, the first partial derivatives of $Q(\boldsymbol{\theta} | \mathbf{x}, \boldsymbol{\theta}^{(p)})$ with respect to μ_a , σ_a^2 and σ^2 are derived, respectively. Then, by equating each derivative to zero, we can obtain

$$\mu_a^{(p+1)} = \frac{1}{\sum_{l=1}^k n_l} \sum_{l=1}^k \sum_{i=1}^{n_l} \mu_{li}^{(p)}, \quad (25)$$

$$\sigma_a^{2(p+1)} = \frac{\sum_{l=1}^k \sum_{i=1}^{n_l} \left(\left[\mu_{li}^{(p)} \right]^2 + \sigma_{li}^{2(p)} - 2\mu_{li}^{(p)} \mu_a^{(p+1)} + \left[\mu_a^{(p+1)} \right]^2 \right)}{\sum_{l=1}^k n_l}, \quad (26)$$

$$\sigma^{2(p+1)} = \frac{\sum_{l=1}^k \sum_{i=1}^{n_l} \left(\mathbf{x}_{li}^T \boldsymbol{\Sigma}_{li}^{-1} \mathbf{x}_{li} - 2\mu_{li}^{(p)} \mathbf{x}_{li}^T \boldsymbol{\Sigma}_{li}^{-1} \boldsymbol{\psi}_{li} + \left(\left[\mu_{li}^{(p)} \right]^2 + \sigma_{li}^{2(p)} \right) \boldsymbol{\psi}_{li}^T \boldsymbol{\Sigma}_{li}^{-1} \boldsymbol{\psi}_{li} \right)}{\sum_{l=1}^k \sum_{i=1}^{n_l} m_{li}}. \quad (27)$$

Note that $\sigma^{2(p+1)}$ depends on the estimates of α_1 , β and H . Hence, by substituting $\mu_a^{(p+1)}$, $\sigma_a^{2(p+1)}$ and $\sigma^{2(p+1)}$ into (24) and maximizing the profile likelihood function, the estimates of $\alpha_1^{(p+1)}$, $\beta^{(p+1)}$ and $H^{(p+1)}$ can be obtained. Subsequently, by substituting $\alpha_1^{(p+1)}$, $\beta^{(p+1)}$ and $H^{(p+1)}$ into (27), the estimate of $\sigma^{2(p+1)}$ can be determined. The iterations are typically stopped when the relative change in parameter estimations drops below a predefined threshold. The complete algorithm is outlined in Algorithm 2.

Algorithm 2: Parameter Estimations Using the EM Algorithm

Step 1. Initialize $\boldsymbol{\theta}^{(0)} = \left[\mu_a^{(0)}, \sigma_a^{(0)}, \alpha_1^{(0)}, \beta^{(0)}, \sigma^{(0)}, H^{(0)} \right]^T$ and ε . Set $p = 0$.

Step 2. Get $\boldsymbol{\theta}^{(p+1)}$ by using the EM algorithm

E-step:

2.1 Calculate $\mu_{li}^{(p)}$ and $\sigma_{li}^{2(p)}$ by using (22) and (23);

M-step:

2.2 Update $\mu_a^{(p+1)}$ and $\sigma_a^{2(p+1)}$ by using (22) and (23);

2.3 Update $\alpha_1^{(p+1)}$, $\beta^{(p+1)}$ and $H^{(p+1)}$ by substituting $\mu_a^{(p+1)}$, $\sigma_a^{2(p+1)}$ and (27) into (24) and maximizing the profile likelihood function through a three-dimensional search;

2.4 Update $\sigma^{2(p+1)}$ by substituting $\alpha_1^{(p+1)}$, $\beta^{(p+1)}$ and $H^{(p+1)}$ into (30).

Step 3. If $\left| \boldsymbol{\theta}^{(p+1)} - \boldsymbol{\theta}^{(p)} \right| \leq \varepsilon$, obtain $\hat{\boldsymbol{\theta}} = \left[\mu_a^{(p+1)}, \sigma_a^{2(p+1)}, \alpha_1^{(p+1)}, \beta^{(p+1)}, \sigma^{2(p+1)}, H^{(p+1)} \right]^T$. Otherwise, go to Step 2.

4 Simulation study

In this section, the proposed method is illustrated through a numerical simulation case. Furthermore, we demonstrate the superiority of the proposed parameter estimation method and the significance of the

proposed ADT model.

4.1 Simulation settings

Detailed information on the constant-stress ADT simulation case is shown in Table 1. The degradation process exhibits short-term memory because $H = 0.1$. Specifically, the sample sizes for each stress level (N) are set as 6 and the measurements for each sample (M) are set as 10.

Table 1 Information for simulation configuration.

Content	Values
Accelerated stress level (Temperature/ $^{\circ}$ C)	80, 100, 120
Normal stress level ($^{\circ}$ C)	40
Degradation model	$X(s, t) = a \exp(\alpha_1 s^*) \cdot t^{\beta} + \sigma B_H(t), a \sim N(\mu_a, \sigma_a^2)$.
Acceleration model	Arrhenius model
Parameter value: $\mu_a, \sigma_a, \alpha_1, \beta, \sigma, H$	1e-5, 2e-6, 2.5, 1.5, 0.1, 0.1
Inspection interval (h)	100
Failure threshold	5

4.2 Results and analysis

In this case, the initial value of θ is taken from the estimations of the two-step MLE method. The terminated threshold ε for the EM algorithm iteration is set as 0.01. Subsequently, according to Algorithm 2, we obtain the estimations of unknown parameters as shown in Table 2. It can be seen that the estimations are basically close to the true values, which shows the effectiveness of the proposed statistical inference method.

Table 2 Estimated results of θ in the simulation case.

Parameters	μ_a	σ_a	α_1	β	σ	H
Values	9.144e-6	9.559e-7	2.286	1.534	0.104	0.073

Furthermore, the predicted deterministic degradation trends, along with the upper and lower boundaries derived from 10000 simulated degradation paths at 90% confidence level under 80 $^{\circ}$ C, 100 $^{\circ}$ C and 120 $^{\circ}$ C are plotted in Fig. 1. As depicted in Fig. 1, the predicted deterministic degradation trends primarily lie in the observed data across all accelerated stress levels, and the boundaries nicely envelope the observations.

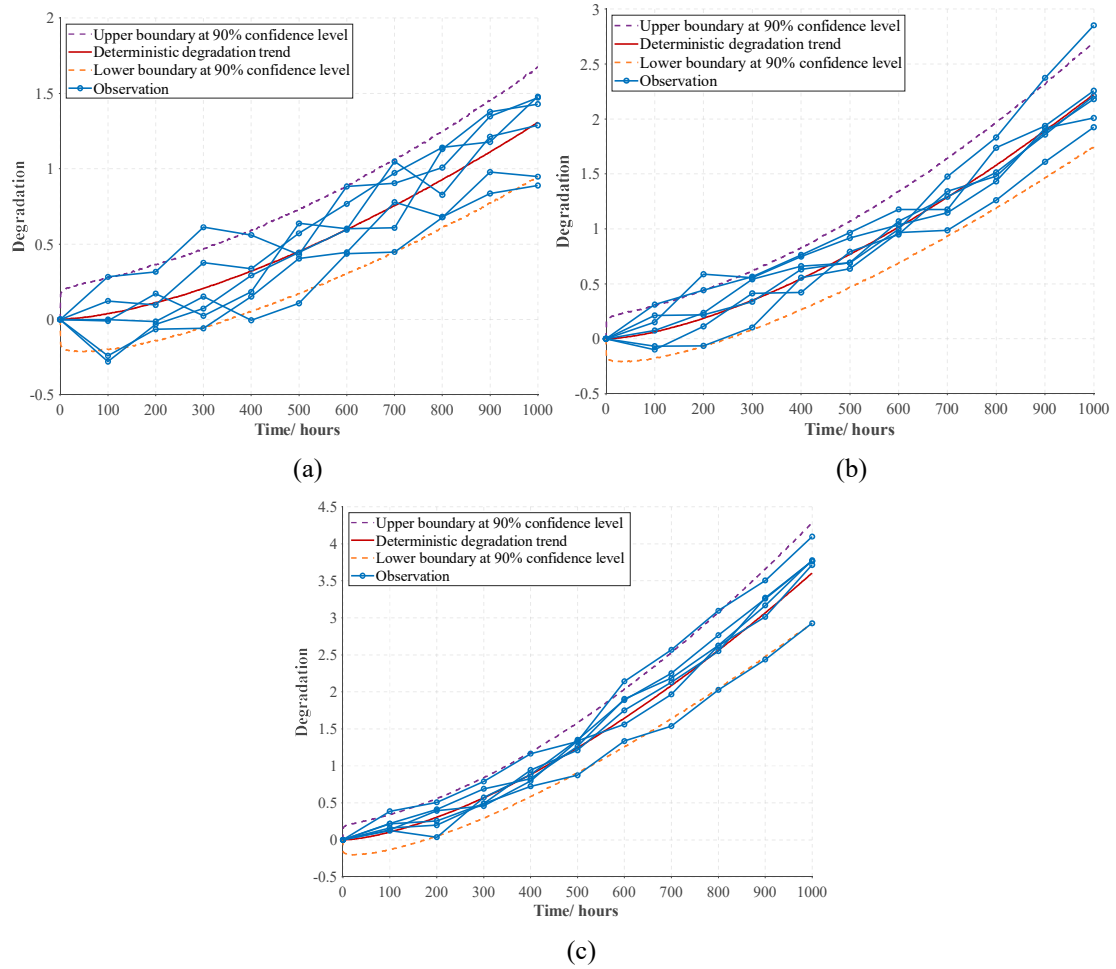


Fig. 1 Deterministic degradation trend, boundaries and observations: (a) 80°C (b) 100°C (c) 120°C.

Then, according to Algorithm 1, when the critical threshold X_{th} is 5, we can estimate the reliability of the product under the normal use condition (40°C) as shown in Fig. 2. From Fig. 2, we can get the reliability of the product for a given operating time. For example, when the product is operated for 4613 hours, its reliability is 0.99. The results can provide guidance for the development of maintenance and warranty strategies.

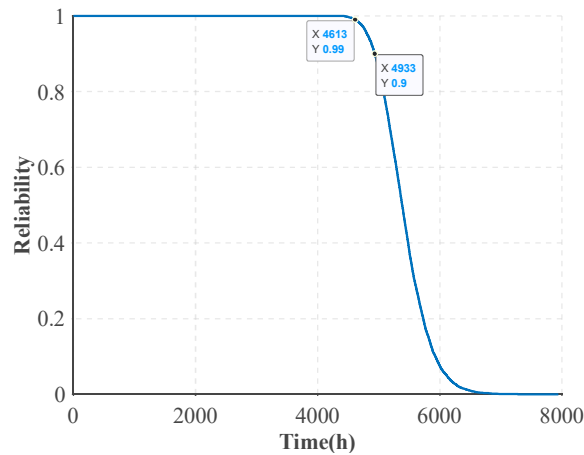


Fig. 2 Reliability of the product under normal stress level (40°C).

4.3 Discussions

4.3.1 Comparison of parameter estimation methods

In order to illustrate the superiority of the proposed statistical inference method compared to the existing two-step MLE method [25, 26], in this subsection, nine combinations of (N, M) are chosen to generate simulated ADT data. Other simulation settings are the same as in Table 1. For each combination, we obtain the parameter estimations by using these two statistical inference methods. Then, we compare the maximum value of the log-likelihood function l_{\max} and the relative errors (RE) between the estimations and the true values. The RE of the parameter estimation is given by

$$RE = \sum \left| \frac{\hat{\theta} - \theta}{\theta} \right|. \quad (28)$$

Obviously, the closer RE is to 0, the higher the accuracy of the parameter estimations.

Table 3 gives the estimations of unknown parameters for two methods under nine combinations of sample sizes and measurements. Fig. 3 illustrates the RE for two methods under different combinations.

From Table 3 and Fig. 3, we can get the following results:

- For the two-step MLE method, when the number of measurements is small, the estimation of H is highly biased. As the number of measurements increases, the estimation of H comes closer to the true value but is still unsatisfactory. On the other hand, for the EM algorithm, when the number of measurements is small, the estimation of H is acceptable. As the number of measurements increases, the estimation of H is very close to the true value. This illustrates the significance of maximizing the overall likelihood function for parameter estimations, especially when degradation process has memory effects and the number of measurements is small.
- As the sample sizes and measurements increase, the RE obtained by these two estimation methods both decreases, indicating that increasing the information from the ADT experiment can improve the accuracy of parameter estimations effectively.
- In all combinations, the l_{\max} and RE obtained by the EM algorithm are better than those of the two-step MLE method, proving the superiority of the proposed statistical inference method.

Table 3 Parameter estimations for two methods under nine combinations of sample sizes and measurements.

(N, M)	Method	μ_a	σ_a	α_1	β	σ	H	l_{\max}	RE
(6,10)	two-step MLE	9.11e-6	1.15e-6	2.24	1.54	0.145	2.94e-8	103.83	2.089
	EM algorithm	9.14e-6	9.55e-7	2.28	1.53	0.104	0.073	105.61	1.025
(6,20)	two-step MLE	1.14e-5	2.65e-6	2.33	1.50	0.151	0.029	146.23	1.757
	EM algorithm	1.14e-5	2.63e-6	2.32	1.50	0.116	0.082	149.29	0.871
(6,30)	two-step MLE	8.85e-6	1.34e-6	2.48	1.51	0.129	0.047	281.19	1.279
	EM algorithm	8.85e-6	1.34e-6	2.48	1.51	0.109	0.079	283.21	0.762
(12,10)	two-step MLE	1.30e-5	2.70e-6	2.12	1.49	0.156	1.13e-8	167.82	2.376
	EM algorithm	1.30e-5	2.64e-6	2.13	1.49	0.138	0.033	169.20	1.830
(12,20)	two-step MLE	1.32e-5	2.55e-6	2.21	1.49	0.138	0.031	357.17	1.781
	EM algorithm	1.32e-5	2.52e-6	2.21	1.49	0.101	0.091	363.95	0.802
(12,30)	two-step MLE	1.11e-5	1.81e-6	2.47	1.49	0.124	0.059	528.11	0.880
	EM algorithm	1.11e-5	1.80e-6	2.47	1.49	0.103	0.096	532.32	0.297

(18,10)	two-step MLE	1.18e-5	2.91e-6	2.29	1.49	0.164	1.58e-8	218.20	2.364
	EM algorithm	1.18e-5	2.72e-6	2.32	1.49	0.091	0.123	228.28	0.946
(18,20)	two-step MLE	9.27e-6	2.15e-6	2.69	1.49	0.154	0.016	495.73	1.610
	EM algorithm	9.27e-6	2.14e-6	2.68	1.49	0.110	0.081	508.61	0.515
(18,30)	two-step MLE	8.72e-6	2.08e-6	2.58	1.50	0.121	0.062	784.70	0.795
	EM algorithm	8.72e-6	2.08e-6	2.58	1.50	0.101	0.098	790.51	0.234

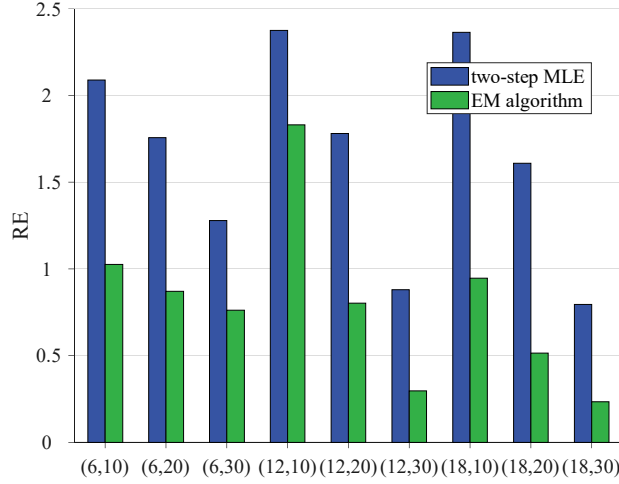


Fig. 3 RE for two estimation methods under nine combinations of sample sizes and measurements.

4.3.2 Comparison of ADT models

The proposed ADT model is described by (8), (9), and (11), which is denoted as M_0 . It should be noted that the proposed ADT model has three special cases as follows:

- When the UtUV is not considered, i.e., a is a constant, it degenerates into the model in [21], which is denoted as M_1 .

$$M_1 : X(s, t) = a \exp(\alpha_1 s^*) t^\beta + \sigma B_H(t). \quad (29)$$

- When the memory effects in the degradation process are not considered, i.e., $H = 0.5$, it degenerates into the model in [25], which is denoted as M_2 .

$$M_2 : X(s, t) = a \exp(\alpha_1 s^*) t^\beta + \sigma B(t), a \sim N(\mu_a, \sigma_a^2). \quad (30)$$

- When the UtUV and the memory effects are both not considered, i.e., a is a constant and $H = 0.5$, it degenerates into the model in [36], which is denoted as M_3 .

$$M_3 : X(s, t) = a \exp(\alpha_1 s^*) t^\beta + \sigma B(t). \quad (31)$$

In order to illustrate the superiority of the proposed ADT model compared to existing ADT models, in this subsection, we set the combination of (N, M) as (12,30) to generate ADT simulation data. Other simulation settings are the same as in Table 1. For the model M_0 and M_2 , the unknown parameters are estimated based on the EM algorithm. For the model M_1 and M_3 , the parameters are obtained by directly maximizing the log-likelihood function. Then, we calculate the l_{\max} and the Akaike information criterion (AIC) for each ADT model. The AIC is expressed as [37]

$$AIC = -2l_{\max} + 2n_p, \quad (32)$$

where n_p is the number of unknown parameters. The smaller the AIC, the better the model fits.

Table 4 gives the estimations of unknown parameters for the four ADT models. Clearly, from l_{\max} and AIC values, M_0 is the most effective model for describing the ADT data, followed by model M_2 , then is model M_1 , and model M_3 is the worst. Analyzing the reasons, the model M_2 and M_1 partially consider the UtUV and the memory effects, respectively. Therefore, they both perform worse than the model M_0 , which considers the UtUV and the memory effects simultaneously. Moreover, model M_1 even gets wrong degradation law, i.e., the degradation process exhibits long-term memory, which is due to the lack of consideration of the UtUV. As for the model M_3 , both the UtUV and the memory effects are not considered, which leads to the poorest fitting results.

Table 4 Parameter estimations for the four ADT models.

Model	μ_a	σ_a	α_1	β	σ	H	l_{\max}	AIC
M_0	1.110e-5	1.802e-6	2.470	1.491	0.103	0.096	532.326	-1052.65
M_1	9.800e-6	/	2.404	1.513	0.013	0.561	308.210	-606.42
M_2	1.031e-5	1.539e-6	2.521	1.495	0.016	/	392.799	-775.60
M_3	9.063e-6	/	2.670	1.501	0.016	/	266.943	-525.89

In addition, the reliability of the product under normal stress level (40°C) for the four ADT models with the real values are illustrated in Fig. 4. It is evident that model M_0 gives the most accurate inference results compared to other ADT models, especially in the high reliability part of concern (i.e., the reliability range from 0.9 to 1), proving the superiority of the proposed ADT model.

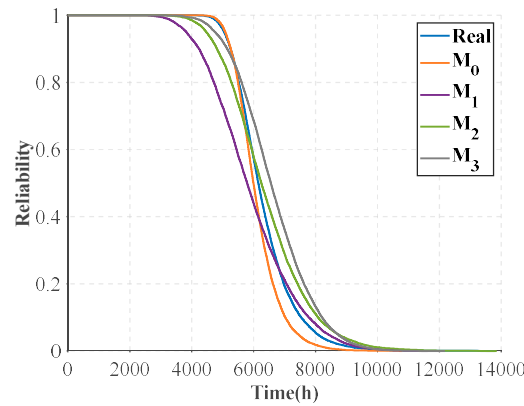


Fig. 4 Reliability of the product under normal stress level (40°C) for the four ADT models with the real values.

5 Engineering application

In this section, we take the accelerated degradation data of microwave electronic assembly to illustrate our method and compare it with other ADT models.

5.1 Data description

A tuner is a long-lifespan microwave electronic assembly designed primarily for reception, filtering, amplification and gain control of cable signals. Previous investigations into tuner failures have shown

the significant impact of temperature on the degradation process [38]. To evaluate the reliability of the tuner, a constant-stress ADT based on temperature was performed under 4 stress levels. And, the key performance parameter, noise, was measured every ten hours by a computerized measuring system. Fig. 5 illustrates detailed degradation data.

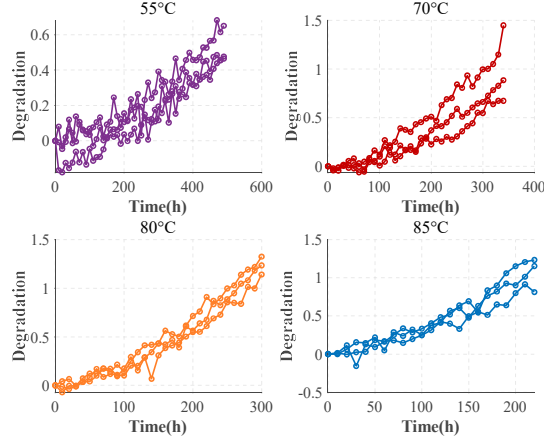


Fig. 5 Accelerated degradation data of microwave electronic assembly under 4 stress levels.

5.2 Modeling and analysis

The Arrhenius model is adopted to build up the acceleration model since the applied accelerated stress is temperature. Then, stress normalization is employed according to (8), where the normal stress level is 20°C. Next, based on the two-step MLE method [25, 26], the initial values of the unknown parameters are set as $\theta^{(0)} = [1e-6, 2e-7, 4, 1.5, 0.01, 1e-7]^T$, and the terminated threshold ε for the EM algorithm iteration is set as 0.01. Subsequently, according to Algorithm 2, we obtain the estimations of unknown parameters as shown in Table 5.

Table 5 Estimated results of θ in the microwave case.

Parameters	μ_a	σ_a	α_1	β	σ	H
Values	1.073e-6	1.894e-7	4.667	1.691	0.073	2.497e-8

From Table 5, it can be deduced that the degradation process of the electronic assembly exhibits short-term memory because $H < 0.5$. The short-term memory effect in the degradation process is also reported in [39]. Besides, it can be found that H is close to zero in our case. At this point, the FBM is close to a logarithmically correlated Gaussian random process [40], which has been studied in financial mathematics [41].

Then, we generate 1000 degradation paths according to the estimations in Table 5. The predicted deterministic degradation trends and boundaries of performance with temperature and time are plotted in Fig. 6 (a). When the critical threshold X_{th} is 7, the performance margin can be calculated according to (12). Fig. 6 (b) illustrates the predicted deterministic degradation trends and boundaries of margin with temperature and time. It can be seen from the above figures that the degradation and corresponding boundary width increase with the increase of time and temperature.

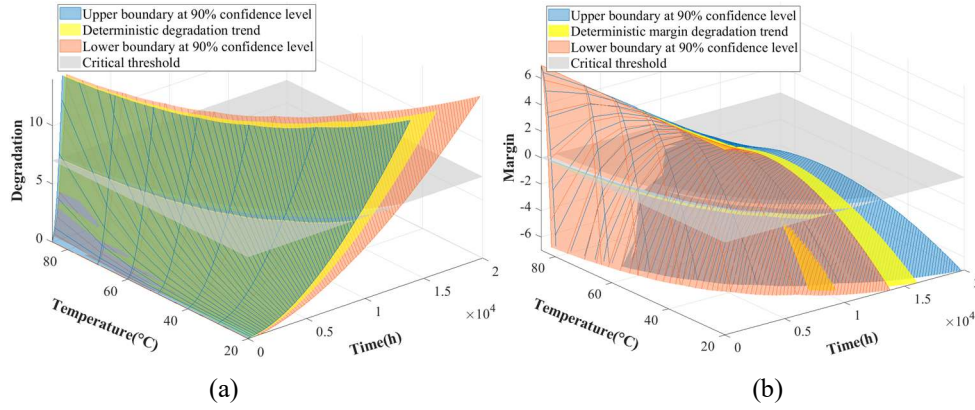


Fig. 6 Deterministic degradation trends and boundaries of microwave electronic assembly performance and margin with temperature and time.

Next, according to Algorithm 1, we can deduce the reliability under different temperature and time as shown in Fig. 7 (a). Specially, the reliability of the electronic assembly under the normal use condition (20°C) are illustrated in Fig. 7 (b). From Fig. 7, we can get some valuable information for the development of maintenance and warranty strategies. For example, when the electronic assembly is operated for 8639 hours, the reliability of the electronic assembly is nearly 0.99.

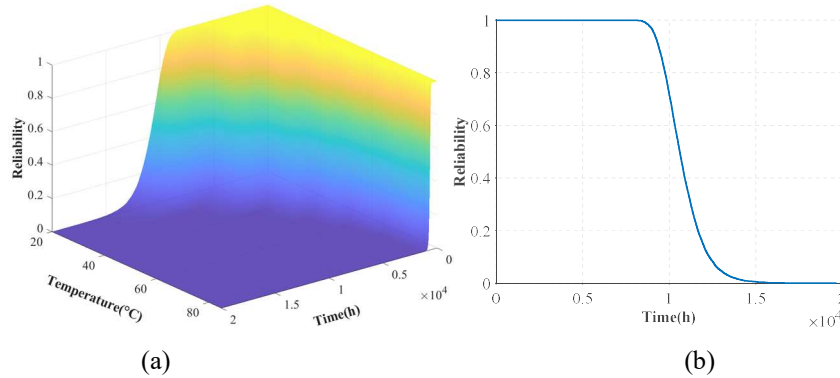


Fig. 7 Reliability of microwave electronic assembly under (a) different temperature and time (b) normal stress level (20°C).

5.3 Discussions

In general, the better the model fits the degradation data, the greater the potential for the model to reflect the degradation law. Besides, it should be recalled that the ultimate goal of modeling ADT data is to extrapolate the lifetime and reliability of the product under the normal use condition, so it is crucial to ensure the accuracy of the degradation prediction for unseen stress levels. To this end, we will discuss the fitting and extrapolation capabilities of the proposed model M_0 compared to other existing ADT models mentioned in Section 4.3.2.

5.3.1 Comparison of model fitting

In this subsection, we first calculate the l_{\max} and the AIC to compare the effectiveness of different ADT models in fitting the degradation data. Table 6 gives the estimations of unknown parameters for the four ADT models. As can be seen in Table 6, from l_{\max} and AIC values, M_0 is the most suitable model

since it considers the UtUV and the short-term memory effect is captured.

Table 6 Parameter estimations for the four ADT models in the microwave case.

Model	μ_a	σ_a	α_1	β	σ	H	l_{\max}	AIC
M_0	1.073e-6	1.894e-7	4.667	1.691	0.073	2.497e-8	579.444	-1146.888
M_1	1.349e-6	/	4.518	1.674	0.056	0.1113	551.784	-1093.568
M_2	1.072e-6	2.113e-8	4.473	1.723	0.023	/	479.348	-948.696
M_3	1.601e-6	/	4.280	1.684	0.023	/	479.483	-950.966

Furthermore, in order to quantitatively compare the performance of different ADT models in describing the real degradation data, we set up three comparison indices \overline{ER} , \overline{ER}^U , and \overline{ER}^L to assess the precision of predicted deterministic degradation trend and uncertainty quantification [42]. Specifically, for each ADT model, we generate 1000 degradation paths according to the estimations in Table 6 and calculate the predicted deterministic degradation trend x_{ij}^{pre} , predicted upper boundary x_{ij}^{pre-U} and predicted lower boundary x_{ij}^{pre-L} at t_{ij} under the l^{th} stress level. Then, the three comparison indices can be calculated as shown in (33), where $\text{mean}\{x_{ij}^{sim}\}_{1 \leq i \leq 1000}$, $\text{quantile}\{x_{ij}^{sim}\}_{5\%}^U$ and $\text{quantile}\{x_{ij}^{sim}\}_{5\%}^L$ denote the mean value, upper 5% quantile and lower 5% quantile for the 1000 simulated degradation paths, respectively.

$$\begin{aligned}
\overline{ER} &= \frac{1}{k} \sum_{i=1}^k \overline{ER}_i, \overline{ER}_i = \frac{1}{n_l} \sum_{j=1}^{m_i} ER_{ij}, \\
ER_{ij} &= \frac{|x_{ij}^{pre} - \bar{x}_{ij}|}{\bar{x}_{ij}}, \bar{x}_{ij} = \frac{1}{n_l} \sum_{j=1}^{m_i} x_{ij}, x_{ij}^{pre} = \text{mean}\{x_{ij}^{sim}\}_{1 \leq i \leq 1000}; \\
\overline{ER}^U &= \frac{1}{k} \sum_{i=1}^k \overline{ER}_i^U, \overline{ER}_i^U = \frac{1}{n_l} \sum_{j=1}^{m_i} ER_{ij}^U, \\
ER_{ij}^U &= \frac{|x_{ij}^{pre-U} - x_{ij}^U|}{x_{ij}^U}, x_{ij}^U = \max_{1 \leq i \leq n_l} \{x_{ij}\}, x_{ij}^{pre-U} = \text{quantile}\{x_{ij}^{sim}\}_{5\%}^U; \\
\overline{ER}^L &= \frac{1}{k} \sum_{i=1}^k \overline{ER}_i^L, \overline{ER}_i^L = \frac{1}{n_l} \sum_{j=1}^{m_i} ER_{ij}^L, \\
ER_{ij}^L &= \frac{|x_{ij}^{pre-L} - x_{ij}^L|}{x_{ij}^L}, x_{ij}^L = \min_{1 \leq i \leq n_l} \{x_{ij}\}, x_{ij}^{pre-L} = \text{quantile}\{x_{ij}^{sim}\}_{5\%}^L.
\end{aligned} \tag{33}$$

Obviously, the closer \overline{ER}_i is to 0, the more accurately the model predicts the deterministic degradation trend under the l^{th} stress level. The closer \overline{ER}_i^U or \overline{ER}_i^L is to 0, the better the predicted boundary can describe the uncertainty of the real data under the l^{th} stress level. Moreover, \overline{ER} , \overline{ER}^U , and \overline{ER}^L reflect the predicted performance of an ADT model under all stress levels.

Table 7 gives the quantitative indices for the four ADT models under all stress levels. The visualization results of the deterministic degradation trend and the degradation boundary are shown in Fig. 8 and Fig. 9.

Table 7 Quantitative indices of the microwave case under all stress levels.

Model	\overline{ER}	\overline{ER}^U	\overline{ER}^L
M_0	0.1335	0.9389	3.7036
M_1	0.1490	1.1209	3.8215
M_2	0.1429	2.3264	12.3555
M_3	0.1849	2.4501	11.3810

Note: The bolded results depict the best ones.

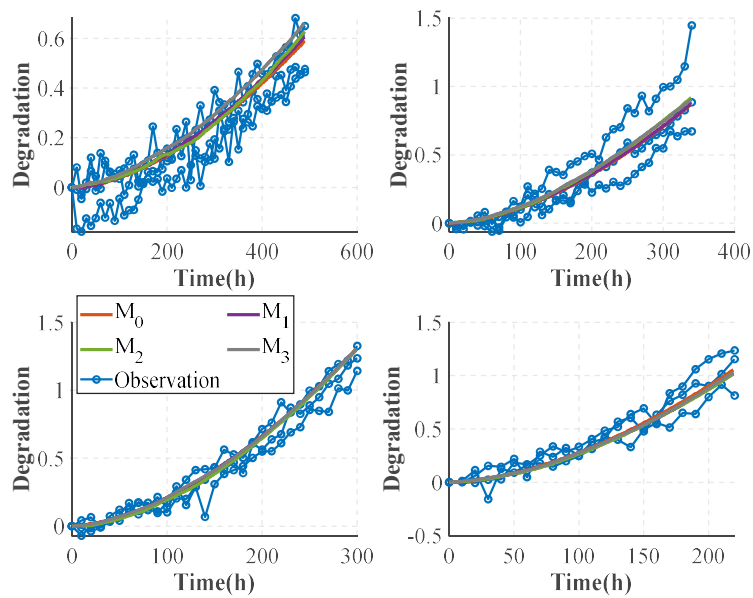


Fig. 8 Prediction for the deterministic degradation trend under all stress levels.

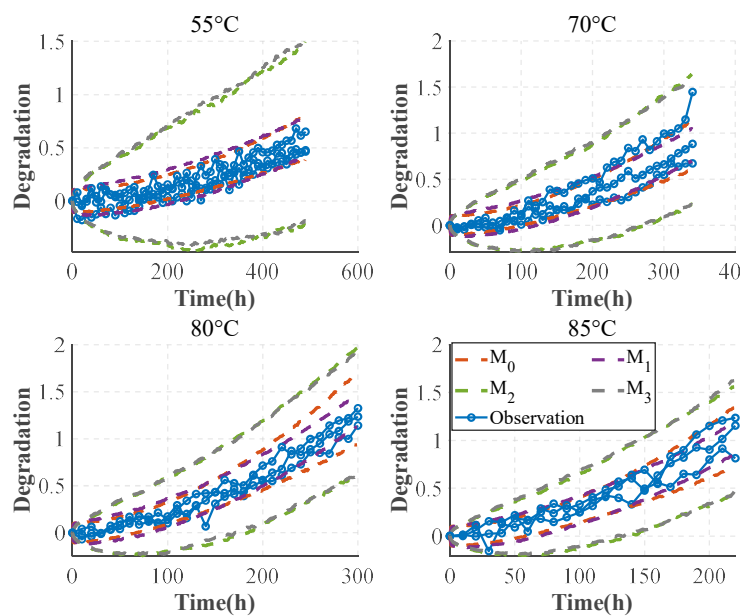


Fig. 9 Prediction for the degradation boundary under all stress levels.

According to the above comparative tables and figures, compared with the other models, M_0 is superior not only in predicting the deterministic degradation, but also in the uncertainty quantification. Additionally, the uncertainty quantification of M_0 and M_1 is considerably superior to that of models M_2 and M_3 , demonstrating the necessity of considering the memory effects in the degradation process.

5.3.2 Comparison of model extrapolation

In this subsection, we develop a cross-validation scheme [43] shown in Table 8 to explore the extrapolation capability of the four ADT models. The results of quantitative indices for the cross-validation 1 and 2 are listed in Table 9 and Table 10, respectively. The visualization results are shown in Fig. 10 and Fig. 11, respectively.

Table 8 Plans of cross-validation

Projects	Training data	Testing data
Cross-validation 1	The data under all stress levels except the lowest stress level	The data under the lowest stress level (55°C)
Cross-validation 2	The data under all stress levels except the highest stress level	The data under the highest stress level (85°C)

Table 9 Quantitative indices of the microwave case for the cross-validation 1.

Model	\overline{ER}_1	\overline{ER}_1^U	\overline{ER}_1^L
M_0	0.2937	0.7971	3.3203
M_1	0.4637	1.2940	1.3456
M_2	0.4973	3.2261	27.1602
M_3	0.3621	3.2290	28.5961

Note: The bolded results depict the best ones.

Table 10 Quantitative indices of the microwave case for the cross-validation 2.

Model	\overline{ER}_4	\overline{ER}_4^U	\overline{ER}_4^L
M_0	0.1249	0.4198	9.8124
M_1	0.2167	0.4468	9.9591
M_2	0.1617	0.8326	11.8889
M_3	0.2153	0.7809	12.5949

Note: The bolded results depict the best ones.

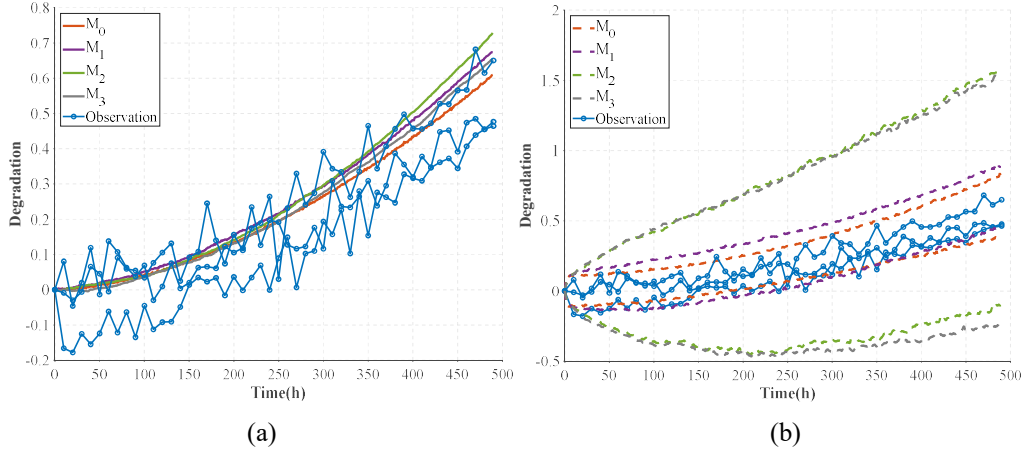


Fig. 10 Prediction for the cross-validation 1: (a) deterministic degradation trend (b) degradation boundary.

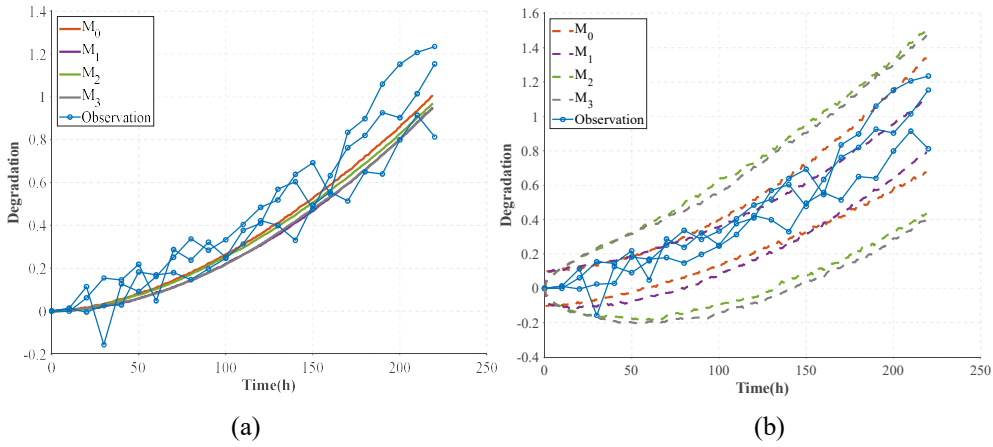


Fig. 11 Prediction for the cross-validation 2: (a) deterministic degradation trend (b) degradation boundary.

From the above comparative tables and figures, the following results can be obtained:

- According to Table 9 and Table 10, for both cross-validations, the predicted deterministic degradation trends based on M_0 consistently outperform others significantly. In terms of uncertainty quantification, the upper and lower boundary predictions based on M_0 are both the best for cross-validation 2, while the lower boundary predictions based on M_0 are worse than those of M_1 for cross-validation 1. Overall, model M_0 has a superior capacity for uncertainty quantification.
- From Fig. 10 and Fig. 11, for both cross-validations, M_0 best describes the deterministic degradation trend and envelopes the real data, proving the superiority of the model M_0 .
- By analyzing the predictions of the four ADT models for two cross-validations, we can deduce that M_0 is more suitable for lifetime and reliability inference under the normal stress level in this case.

6 Conclusion

This paper seeks to tackle the challenges of reliability modeling and statistical analysis of ADT data

with memory effects and UtUV. The following conclusions are drawn from this paper:

- This paper proposes a comprehensive degradation model considering the influence of external stresses, memory effects and UtUV. The memory effects are quantified by the Hurst exponent in the FBM and the UtUV is quantified in the acceleration model. Besides, a statistical inference method based on the EM algorithm is devised to ensure the maximization of the overall likelihood function.
- The results of the simulation case illustrate that the memory effect estimation of the proposed statistical inference method is more accurate than the two-step MLE method, especially when the number of measurements is small. Moreover, if the sample difference is large, the memory effect estimation is highly biased of the ADT model without considering UtUV, deviating from the actual degradation law.
- A microwave case is utilized to demonstrate the efficacy of the proposed methodology. Findings show that ADT models considering memory effects are superior in uncertainty quantification. Besides, the proposed model gives superior predictions in both deterministic degradation trends and uncertainty quantification compared to the existing ADT models.

Beyond the scope of this study, there exists additional issues that warrant investigation in future research. For example, we only focus on modeling constant-stress ADT data in this work. Constructing an ADT model considering memory effects for the step-stress ADT data is an interesting topic and worth further research.

Declarations of interest

None.

Acknowledgements

This work was supported by the National Natural Science Foundation of China [grant number 51775020], the Science Challenge Project [grant number. TZ2018007], the National Natural Science Foundation of China [grant numbers 62073009].

References

- [1]Ye Z.S., Xie M. Stochastic modelling and analysis of degradation for highly reliable products. *Applied Stochastic Models in Business and Industry*. 2015, 31(1): 16-32.
- [2]Charki A., Laronde R., Bigaud D. Accelerated degradation testing of a photovoltaic module. *Journal of photonics for energy*. 2013, 3(1): 033099-033099.
- [3]Santini T., Morand S., Fouladirad M., et al. Accelerated degradation data of SiC MOSFETs for lifetime and Remaining Useful Life assessment. *Microelectronics Reliability*. 2014, 54(9): 1718-1723.
- [4]Yan W., Riahi H., Benzarti K., et al. Durability and Reliability Estimation of Flax Fiber Reinforced Composites Using Tweedie Exponential Dispersion Degradation Process. *Mathematical Problems in Engineering*. 2021, 2021: 6629637.
- [5]Liu Z., Li X., Kang R. Uncertain differential equation based accelerated degradation modeling. *Reliability Engineering and System Safety*. 2022, 225.
- [6]Wang C., Liu J., Yang Q., et al. Recoverability effects on reliability assessment for accelerated

degradation testing. *IIEE Transactions*. 2023, 55(7): 698-710.

[7]Jiang P., Wang B., Wang X., et al. Inverse Gaussian process based reliability analysis for constant-stress accelerated degradation data. *Applied Mathematical Modelling*. 2022, 105: 137-148.

[8]Zhang H., Zhou D., Chen M., et al. FBM-Based Remaining Useful Life Prediction for Degradation Processes With Long-Range Dependence and Multiple Modes. *IEEE Transactions on Reliability*. 2018.

[9]Guérin T., Levernier N., Bénichou O., et al. Mean first-passage times of non-Markovian random walkers in confinement. *Nature*. 2016, 534(7607): 356-359.

[10]Giorgio M., Guida M., Pulcini G. A new class of Markovian processes for deteriorating units with state dependent increments and covariates. *IEEE Transactions on Reliability*. 2015, 64(2): 562-578.

[11]Giorgio M., Pulcini G. A new age- and state-dependent degradation process with possibly negative increments. *Quality and Reliability Engineering International*. 2019, 35(5): 1476-1501.

[12]Peng W., Zhu S.-P., Shen L. The transformed inverse Gaussian process as an age-and state-dependent degradation model. *Applied Mathematical Modelling*. 2019, 75: 837-852.

[13]Duan F., Wang G. Bayesian analysis for the transformed exponential dispersion process with random effects. *Reliability Engineering & System Safety*. 2022, 217: 108104.

[14]Sottinen T. Fractional Brownian motion, random walks and binary market models. *Finance and Stochastics*. 2001, 5(3): 343-355.

[15]Burnecki K., Kepten E., Janczura J., et al. Universal algorithm for identification of fractional Brownian motion. A case of telomere subdiffusion. *Biophysical Journal*. 2012, 103(9): 1839-1847.

[16]Zhang H., Chen M., Shang J., et al. Stochastic process-based degradation modeling and RUL prediction: from Brownian motion to fractional Brownian motion. *Science China Information Sciences*. 2021, 64(7).

[17]Xi X., Chen M., Zhou D. Remaining Useful Life Prediction for Degradation Processes with Memory Effects. *IEEE Transactions on Reliability*. 2017, 66(3): 751-760.

[18]Xi X., Chen M., Zhang H., et al. An improved non-Markovian degradation model with long-term dependency and item-to-item uncertainty. *Mechanical Systems and Signal Processing*. 2018, 105: 467-480.

[19]Shao Y., Si W. Degradation Modeling With Long-Term Memory Considering Measurement Errors. *IEEE Transactions on Reliability*. 2021.

[20]Xi X., Zhou D., Chen M., et al. Remaining useful life prediction for multivariable stochastic degradation systems with non-Markovian diffusion processes. *Quality and Reliability Engineering International*. 2020, 36(4): 1402-1421.

[21]Si W., Shao Y., Wei W. Accelerated Degradation Testing with Long-Term Memory Effects. *IEEE Transactions on Reliability*. 2020, 69(4): 1254-1266.

[22]Wu J.-P., Kang R., Li X.-Y. Uncertain accelerated degradation modeling and analysis considering epistemic uncertainties in time and unit dimension. *Reliability Engineering and System Safety*. 2020, 201: 106967.

[23]Jiang P. Statistical Inference of Wiener Constant-Stress Accelerated Degradation Model with Random Effects. *Mathematics*. 2022, 10(16): 2863.

[24]Zheng H., Yang J., Kang W., et al. Accelerated degradation data analysis based on inverse Gaussian

- process with unit heterogeneity. *Applied Mathematical Modelling*. 2024, 126: 420-438.
- [25]Tang S., Guo X., Yu C., et al. Accelerated degradation tests modeling based on the nonlinear wiener process with random effects. *Mathematical Problems in Engineering*. 2014, 2014.
- [26]Liu L., Li X., Sun F., et al. A general accelerated degradation model based on the wiener process. *Materials*. 2016, 9(12).
- [27]Dempster A.P., Laird N.M., Rubin D.B. Maximum likelihood from incomplete data via the EM algorithm. *Journal of the royal statistical society: series B (methodological)*. 1977, 39(1): 1-22.
- [28]Mandelbrot B.B., Van Ness J.W. Fractional Brownian motions, fractional noises and applications. *SIAM Review*. 1968, 10(4): 422-437.
- [29]Escobar L.A., Meeker W.Q. A review of accelerated test models. *Statistical Science*. 2006. 552-577.
- [30]Ye Z.S., Chen L.P., Tang L.C., et al. Accelerated degradation test planning using the inverse gaussian process. *IEEE Transactions on Reliability*. 2014, 63(3): 750-763.
- [31]Ye X., Hu Y., Zheng B., et al. A new class of multi-stress acceleration models with interaction effects and its extension to accelerated degradation modelling. *Reliability Engineering and System Safety*. 2022, 228.
- [32]Kang R. *Belief reliability theory and methodology*. Singapore: Springer, 2021.
- [33]Wood A.T., Chan G. Simulation of stationary Gaussian processes in $[0, 1]$ d. *Journal of computational and graphical statistics*. 1994, 3(4): 409-432.
- [34]Li H., Pan D., Chen C.L.P. Reliability modeling and life estimation using an expectation maximization based wiener degradation model for momentum wheels. *IEEE Transactions on Cybernetics*. 2015, 45(5): 969-977.
- [35]Pan D., Wei Y., Fang H., et al. A reliability estimation approach via Wiener degradation model with measurement errors. *Applied Mathematics and Computation*. 2018, 320: 131-141.
- [36]Liao C.M., Tseng S.T. Optimal design for step-stress accelerated degradation tests. *IEEE Transactions on Reliability*. 2006, 55(1): 59-66.
- [37]Cavanaugh J.E., Neath A.A. The Akaike information criterion: Background, derivation, properties, application, interpretation, and refinements. *Wiley Interdisciplinary Reviews: Computational Statistics*. 2019, 11(3): e1460.
- [38]Sun F., Fu F., Liao H., et al. Analysis of multivariate dependent accelerated degradation data using a random-effect general Wiener process and D-vine Copula. *Reliability Engineering & System Safety*. 2020, 204: 107168.
- [39]Zhang H., Jia C., Chen M. Remaining Useful Life Prediction for Degradation Processes with Dependent and Nonstationary Increments. *IEEE Transactions on Instrumentation and Measurement*. 2021, 70.
- [40]Fyodorov Y., Khoruzhenko B., Simm N. Fractional Brownian motion with Hurst index $H=0$ and the Gaussian unitary ensemble. 2016.
- [41]Fyodorov Y.V., Doussal P.L. Moments of the position of the maximum for GUE characteristic polynomials and for log-correlated Gaussian processes. *Journal of Statistical Physics*. 2016, 164(1): 190-240.
- [42]Li X.Y., Chen D.Y., Wu J.P., et al. 3-Dimensional general ADT modeling and analysis: Considering

epistemic uncertainties in unit, time and stress dimension. *Reliability Engineering and System Safety*. 2022, 225.

[43]Shao J. Linear model selection by cross-validation. *Journal of the American Statistical Association*. 1993, 88(422): 486-494.